Point defect properties of the $VCrMnFe_{0.33}$ multi-principal alloy from first-principles calculations

Shuang Lyu[a], Yue Chen[a*]

[a] Department of Mechanical Engineering, The University of Hong Kong, Pokfulam Road, Hong Kong SAR, China

Email address: yuechen@hku.hk

Abstract

We performed first-principles calculations to explore the point defect formation and migration properties and the corresponding chemical environment effects for a bcc $VCrMnFe_{0.33}$ multi-principal alloy. The results indicate that the mean vacancy formation energies are higher than those of other face-centered cubic (fcc) alloys, and vacancies favor Mn-rich surrounding environments. The exchange between vacancies and V atoms presents lower energy barriers due to the large atomic size of V. Moreover, interstitial calculations found that [110] direction dumbbells take up more than 93%, suggesting a slow defect diffusion. The large V interstitials can substitute neighboring atoms and leave the squeezed atom forming dumbbells with its surroundings. Our investigation indicates that this low-activation multi-principal alloy may exhibit promising irradiation resistance due to its special defect properties.

Keywords: Multi-principal alloys; Defect properties; First-principles calculations; Local chemical environment

1 Introduction

Stainless steels are widely used in the nuclear industry due to their good thermomechanical properties[1]. However, the development of new-generation fission raises new challenges for reactors in extreme irradiation environments. Under continuous high-energy particle irradiation, atoms can be displaced from initial lattice sites, thereby forming vacancies and interstitial defects. The primarily formed point defects can evolve into defect clusters, void swelling, degrade material properties and reduce lifetimes[2, 3]. The generation and mobility of point defects must be examined to understand the underlying mechanism of irradiation.

High entropy alloys (HEAs) are composed of multi-principal elements and have recently been reported to have improved radiation damage tolerance[4, 5]. A reduced fraction of large-size defect damage in multi-principal alloys NiCoCr and NiCoCrFe has been reported[5, 6]; no sign of an irradiation-induced dislocation loop was observed in a tungsten-based HEA, even after 8 dpa radiation[7]. Lu[8] attributed the improved irradiation resistance of NiCoCrFe HEA to the enhanced point defect recombination resulting from tailored defect cluster motion from the long-range one-dimensional mode to the short-range three-dimensional mode. Moreover, the atomic disorder and corresponding lattice distortion of HEAs are reported to mitigate energy dissipation and damage

accumulation, thus improving the irradiation tolerance performance[9, 10]. The enhanced irradiation resistance suggests that multi-principal alloys can be promising materials for nuclear industry applications.

Compared with the experimental difficulty in precisely measuring point defect properties, density functional theory (DFT) provides powerful tools for fundamentally understanding defect generation and diffusion mechanisms[11]. Recent studies based on DFT about point defect properties have mainly concentrated on face-centered cubic (fcc) multi-principal alloys[3, 12-14]. Body-centered cubic (bcc) HEAs have been reported to have no radiation hardening effect and a lower density of helium bubbles after irradiation experiments[7, 15], while there is noticeable radiation hardening in fcc HEAs[16], which indicates that it is essential to evaluate defect properties in bcc multi-principal alloys[17]. Moreover, the neutron activation level of component elements is a crucial criterion that needs consideration[18]. Gilbert et al. predicted the time required for each element to reach low-level activity waste after exposure in a fusion reactor and found that the time for V, Cr, Mn, and Fe was less than 100 years[19]. VCrMnFe alloy has been reported to have a bcc structure with reduced activation[18, 20]. However, defect properties, which can reveal irradiation tolerance at the early stage, have not been systemically studied.

In this work, we carried out a series of first-principles calculations to investigate the formation and migration energies of point defects in a bcc multi-principal alloy composed of V, Cr, Mn, and Fe. Compared with pure metals and other fcc alloys, slower vacancy diffusion and more difficult interstitial dumbbell formation have been demonstrated. The influence of the corresponding chemical environment is also discussed. The present investigation of point defects presents a basic understanding of the irradiation property of $VCrMnFe_{0.33}$.

2 Computational details

Oh et al. [21] revealed that lattice distortion from random atomic distribution can significantly influence HEA properties. Therefore, the special quasi-random structure (SQS) method[22] is applied to describe defect structures. The SQS is constructed via mcsqs, a Monte Carlo generator in the Alloy Theoretic Automated Toolkit (ATAT) [22, 23].

Supercell size is an essential factor in balancing calculation accuracy and computational cost. A previous study found that a 108-atom supercell is sufficient for quaternary alloy calculation[24]. In this work, a 4×4×4 supercell with a total of 128 atoms (39, 39, 38 and 12 atoms of V, Cr, Mn and Fe, respectively) is constructed for defect property investigation.

Based on density functional theory (DFT), we carried out ab initio calculations using the Vienna ab initio simulation package (VASP)[25, 26], with the projector augmented wave (PAW)[27, 28] approach generated pseudopotentials. The generalized gradient approximation parameterized by Perdew, Burke, and Ernzerhof (PBE) [29] was adopted to describe the exchange-correlation interactions. A cutoff energy of 400 eV and a 2×2×2 Γ-centered k-point mesh were used during structure optimization and energy calculation. The spin-polarization effects were taken into consideration in all calculations. The energy and force convergence criteria were set to 1×10^{-4} eV and 1×10^{-3} eV/Å, respectively.

Vacancies and interstitials are introduced by removing or inserting atoms in the supercell. The defect

formation energy can be calculated by Equation (1):

$$E_f = E_d - E_0 \pm \mu_d \quad (1)$$

where E_d and E_0 are the energies for defective and defect-free supercells, respectively. Full relaxation is performed for the defect-free structure, and only atomic positions are optimized while keeping the volume fixed after defects are introduced [24, 30-32]. μ_d is the elemental chemical potential of the defect species *d*. The positive sign is for interstitial defects, while the negative sign is for vacancy defects.

The migration barriers for defects were calculated by the climbing-image nudged elastic band (CI-NEB)[33] methodology, in which three images were interpolated between the initial and final configurations. The energy barriers were determined after the forces on each image converged to 0.01 eV/Å.

3 Results and discussion

3.1 Vacancy formation energy

For point defect investigation, vacancies are generally created by removing an atom from its initial lattice sites in pure metals, which can also be applied in multi-principal alloys. This study considers all possible vacancy sites in the constructed SQS. Vacancy formation energies (E_f^v) grouped by atom type removed are shown in Figure 1, ranging from 1.83 to 3.15 eV. The results is different from pure metal, of which the vacancy formation energy is a constant value[11]. As discussed in previous studies, the variation can be attributed to the chemical environment fluctuation around a vacancy [13, 17].

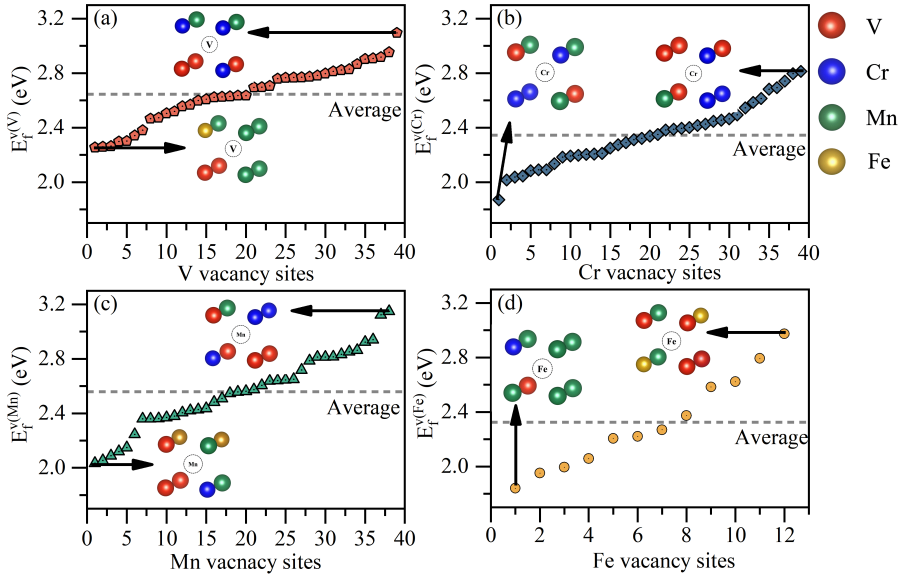

Figure 1. Vacancy formation energies distribution grouped by vacancy types, (a)-(d) for V, Cr, Mn, and Fe, respectively. The data are arranged in ascending order. The inserted configurations present 1NN atomic environments for vacancies with the highest and lowest formation energies.

Table 1. Vacancy formation energy in multi-principal bcc $VCrMnFe_{0.33}$ alloy and pure elemental

metals.

Vacancy formation energy (eV)	$VCrMnFe_{0.33}$					Elemental bcc metals	
	Distribution (%)				Average	This study	Literature
	<2	2.0-	2.5-	>3.0			
V	0	23.08	74.36	2.56	2.65	2.23	2.48[11]
Cr	2.57	76.92	20.51	0	2.34	2.85	2.71[34],
Mn	0	42.11	52.63	5.26	2.56	-0.52	-0.32[11]
Fe	25	41.67	33.33	0	2.32	2.11	2.15[34],

The average vacancy formation energies in the multi-principal bcc $VCrMnFe_{0.33}$ alloy, as well as in pure elemental metals, are summarized in Table 1. The calculated results for pure metals are consistent with previous studies[11, 31, 34]. The mean vacancy formation energies for V, Mn, and Fe in HEA are higher than those in the corresponding pure metals. Although Cr's average vacancy formation energy in $VCrMnFe_{0.33}$ alloy is lower than that in Cr bcc metal, it is higher than those of the other three pure metals. From Table 1, no vacancy formation energy below 2.0 eV is observed for V and Mn vacancies; more than half are higher than 2.5 eV, suggesting that it is more difficult for V and Mn to form vacancy defects.

In addition to pure metals, the vacancy formation energies in $VCrMnFe_{0.33}$ HEA are much higher than those of some fcc multi-principal alloys, including quinary alloys[3, 14], indicating that vacancies are less likely to form in this bcc alloy. A higher vacancy formation energy means more energy consumption for removing an atom from its lattice site. In addition, a lower vacancy formation energy can result in a higher equilibrium vacancy concentration under an irradiation environment, as seen from Equation (2)[32, 35, 36].

$$c_v(T) = c_v^0 exp\ (-\frac{E_f^v}{K_B T}) \tag{2}$$

where $c_v^0 = \exp(-\frac{S_f^v}{K_B})$, K_B is the Boltzmann constant, E_f^v and S_f^v are the vacancy formation energy and entropy, respectively, and S_f^v is on the order of one to a few K_B. Thus, E_f^v determines the equilibrium concentration of vacancies.

Next, first-nearest-neighbor (1NN) atoms around a vacancy are analyzed to investigate how the chemical environment influences vacancy formation. Figure 2 shows the relations between the number of 1NN V, Cr, Mn, and Fe atoms and the vacancy formation energies. Although there is no significant dependence of vacancy formation energy on the 1NN numbers of different atoms, a negative and a positive correlation can be found with the numbers of 1NN Mn and V atoms, respectively. Moreover, from the 1NN environment around different vacancies with the lowest and highest formation energies presented in Figure 1, we find that the lowest formation energy indeed corresponds to vacancies with Mn-rich environments, suggesting a preference for vacancy formation in Mn-rich regions.

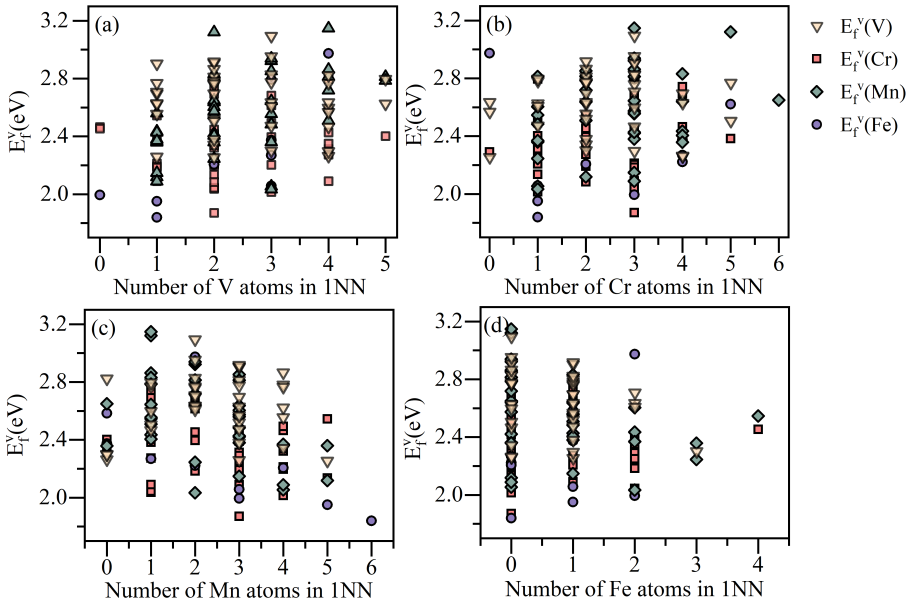

Figure 2. E_f^v variation with respect to the number of V, Cr, Mn, and Fe atoms in the 1NN shell of the vacancy.

3.2 Vacancy migration energy

Vacancy migration is the next step for defect evolution, controlling diffusion kinetics. To explore the diffusion mechanism of vacancies, we calculated migration barriers in $VCrMnFe_{0.33}$ HEA via the CI-NEB method. The migration of a vacancy to its neighboring lattice site is equivalent to the adjacent atom moving to the vacancy site. Four initial vacancy configurations are chosen to investigate the energy evolution for the migration of their eight 1NN atoms, as presented in Figure 3. Different from pure metals, for which the highest energy barrier is always observed at the midpoint of diffusion path, the location of the highest energy barrier in multi-principal element alloys can change significantly due to different atomic displacements from chemical fluctuations.

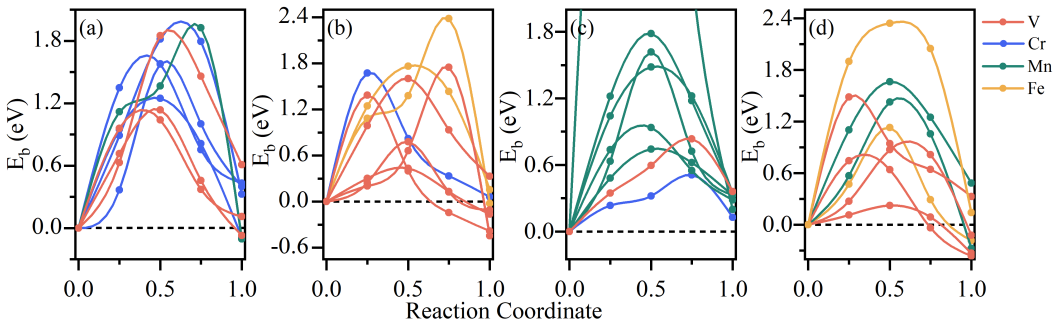

Figure 3. Energy barriers for atoms migrating to neighboring vacancy sites. (a), (b), (c), and (d) correspond to four different vacancy sites.

In Figure 3 (a), four Cr atoms, three V atoms, and one Mn atom are in the 1NN sites of the vacancy. The energy barriers for different V atoms that migrate to the same vacancy vary significantly (from 1.04 to 1.85 eV) and are similar for the four Cr atoms. Consistent results also appear in the other

three vacancies, as Figure 3 (b)-(d) show. This indicates that the migration barriers can be affected not only by the type of the migrating atom, but also by its chemical environment. Specifically, for the vacancy site in Figure 3 (c), the migration barrier for one Mn atom reaches 5.89 eV, indicating the difficulty of migration.

Based on the four selected vacancy sites, the average energy barriers for the migration of V, Cr, Mn, and Fe atoms are 1.04, 1.40, 1.38, and 1.59 eV, respectively. Note that the migration energy barriers are only 0.62, 0.91, and 0.67 eV in V, Cr, and Fe bcc metals, respectively[37, 38]. The enhanced migration energy barriers in the multi-principal $VCrMnFe_{0.33}$ alloy indicate lower vacancy-atom exchange frequencies.

3.3 Formation energy of interstitial defects

For the formation energy of interstitial defects, we insert an atom in the octahedral interstitial site and perform atomic relaxation. Among the 80 interstitials investigated, more than 95% are found to form dumbbells, indicating that dumbbell defects are most common in the bcc $VCrMnFe_{0.33}$ alloy, consistent with previous studies[17]. In the two remaining interstitials, the inserted atoms stay at their initial sites after relaxation with higher formation energies (8.58 eV and 9.32 eV), making these defects unstable and more difficult to form.

Table 2. Probabilities of formation of different interstitial dumbbell formed and the corresponding average formation energies

Dumbbell type	Probability (%)	Average formation energy (eV)
Mn-Fe	21.79	4.22
Mn-Cr	17.95	4.55
Mn-Mn	16.67	4.14
Fe-Cr	16.67	4.56
Mn-V	7.69	4.97
Fe-V	7.69	4.91
Fe-Fe	6.41	4.15
Cr-Cr	2.56	4.73
Cr-V	1.28	4.54
V-V	1.28	5.44

The distribution of the calculated formation energies for stable dumbbells is given in Figure 4 (a), with a mean value of 4.45 eV. The interstitial formation energy spans from 3.31 to 6.24 eV, with the minimum value higher than the highest vacancy formation energy as shown in Figure 1 (3.15 eV), suggesting that vacancies can form more easily than interstitial defects.

Approximately 93% of the calculated dumbbells are in the [110] direction, the same as in pure Cr and Fe, but different from V, where [111] dumbbells form more easily [34, 37]. Compared with the [111] orientated dumbbells, which can easily translate along the dumbbell axis direction, the migration of [110] dumbbells requires a series of rotation and translation jumps[39]. The three-dimensional migration of [110] dumbbells require a relatively high activation energy; thus, interstitial diffusion will be mitigated, resulting in a delayed interstitial evolution under radiation environment.

Figure 4 (b) and Table 2 present the dumbbell formation energy grouped by dumbbell types, from which we can see that Mn-containing dumbbells take up approximately 64%. Mn shows attractive solute-solute interactions in bcc Fe due to its easy magnetism moment changes to adapt to the local chemical environment[3, 40]. The flexible magnetism of Mn may contribute to the significant Mn-containing dumbbells. In contrast, although the V concentration is three times that of Fe, V-related dumbbells are seldom observed after relaxation, and they are fewer than Fe-related dumbbells. From the average formation energies of different types of dumbbells, as shown in Table 2, we find that V-related dumbbells show relatively higher values, indicating that V-containing dumbbells are more difficult to stabilize, which may be due to the largest atomic size of V among the four components.

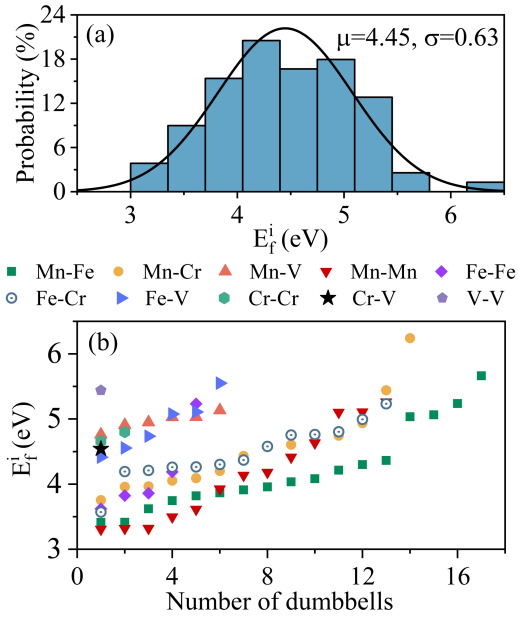

Figure 4. Formation energies of interstitial dumbbells. (a) Distribution of dumbbell formation energies; (b) Formation energies grouped by dumbbell types.

It is found that although a V interstitial atom is inserted, the resulting dumbbells can be non-V-containing. This observation motivates us to investigate how interstitial atoms behave during structural relaxation. In addition to forming dumbbells with the 1NN atoms, the inserted atoms can also knock out its neighboring atoms and behave as substitutes; then, the squeezed atom then combines with its surrounding atoms to form dumbbells, as illustrated in Figure 5(b). This indirect way of dumbbells formation usually occurs when the interstitial atom is V, which has the largest atom size among the four elements. Interstitial V can take up the neighboring atomic site, rather than sharing a lattice site with another atom to form a dumbbell. This is consistent with the results shown in Table 2, in which fewer V-related dumbbells are observed.

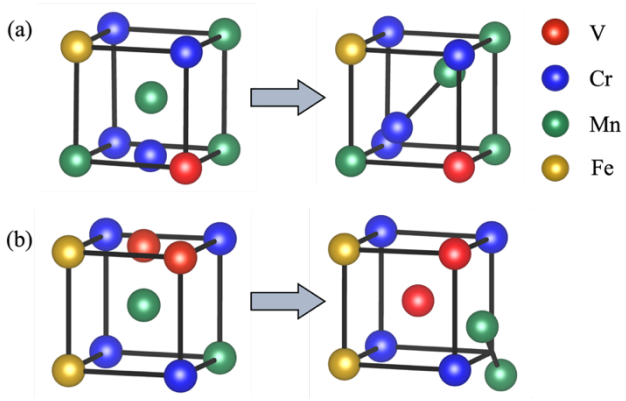

Figure 5. Two ways for dumbbell formation after introducing interstitial atoms. (a) Combines directly with the 1NN atom to form a dumbbell; (b) Substitutes its neighboring atom, and the extruded atom forms a dumbbell with its neighbors.

4 Conclusion

In this study, first-principles calculations were conducted to explore the point defect properties, including vacancies and interstitials, of a $VCrMnFe_{0.33}$ multi-principal alloy. The vacancy formation energy in this bcc alloy is much higher than that in fcc multi-principal alloys reported in the literature. Vacancies with Mn-rich 1NN chemical environments are found to be easier to form in $VCrMnFe_{0.33}$. The calculation of the vacancy migration energy shows a slower vacancy diffusion compared with pure metals, and the vacancies tend to migrate to the neighboring V lattice sites. For the interstitial defects, we find that a majority of the formed dumbbells are in the [110] direction and are Mn-related. V can substitute neighboring atoms, leaving the squeezed atom to develop dumbbells with its neighboring atoms.

Data availability

The DFT calculations were performed with the Vienna ab initio simulation package. All the other codes that support the findings of this study are available from corresponding author upon reasonable request.

Acknowledgements

This work is supported by the National Key Research and Development Program of China (2019YFA0209904). The authors are grateful for the research computing facilities offered by ITS, HKU.

References

[1] R. Klueh and A. T. Nelson, "Ferritic/martensitic steels for next-generation reactors," *Journal of nuclear materials,* vol. 371, no. 1-3, pp. 37-52, 2007.

[2] S. J. Zinkle and J. T. Busby, "Structural materials for fission & fusion energy," (in English),

Materials Today, vol. 12, no. 11, pp. 12-19, Nov 2009, doi: Doi 10.1016/S1369-7021(09)70294-9.

[3] H. Guan, S. Huang, J. Ding, F. Tian, Q. Xu, and J. Zhao, "Chemical environment and magnetic moment effects on point defect formations in CoCrNi-based concentrated solid-solution alloys," *Acta Materialia,* vol. 187, pp. 122-134, 2020, doi: 10.1016/j.actamat.2020.01.044.

[4] M.-R. He *et al.*, "Enhanced damage resistance and novel defect structure of CrFeCoNi under in situ electron irradiation," *Scripta Materialia,* vol. 125, pp. 5-9, 2016, doi: 10.1016/j.scriptamat.2016.07.023.

[5] Y. Lin *et al.*, "Enhanced radiation tolerance of the Ni-Co-Cr-Fe high-entropy alloy as revealed from primary damage," *Acta Materialia,* vol. 196, pp. 133-143, 2020, doi: 10.1016/j.actamat.2020.06.027.

[6] F. Granberg *et al.*, "Mechanism of Radiation Damage Reduction in Equiatomic Multicomponent Single Phase Alloys," *Phys Rev Lett,* vol. 116, no. 13, p. 135504, Apr 1 2016, doi: 10.1103/PhysRevLett.116.135504.

[7] O. El-Atwani *et al.*, "Outstanding radiation resistance of tungsten-based high-entropy alloys," *Sci Adv,* vol. 5, no. 3, p. eaav2002, Mar 2019, doi: 10.1126/sciadv.aav2002.

[8] C. Lu *et al.*, "Enhancing radiation tolerance by controlling defect mobility and migration pathways in multicomponent single-phase alloys," *Nat Commun,* vol. 7, p. 13564, Dec 15 2016, doi: 10.1038/ncomms13564.

[9] Y. Zhang *et al.*, "Influence of chemical disorder on energy dissipation and defect evolution in concentrated solid solution alloys," *Nat Commun,* vol. 6, p. 8736, Oct 28 2015, doi: 10.1038/ncomms9736.

[10] Y. Zhang *et al.*, "Influence of chemical disorder on energy dissipation and defect evolution in advanced alloys," *Journal of Materials Research,* vol. 31, no. 16, pp. 2363-2375, 2016, doi: 10.1557/jmr.2016.269.

[11] S.-L. Shang *et al.*, "A comprehensive first-principles study of pure elements: Vacancy formation and migration energies and self-diffusion coefficients," *Acta Materialia,* vol. 109, pp. 128-141, 2016, doi: 10.1016/j.actamat.2016.02.031.

[12] M. Mizuno, K. Sugita, and H. Araki, "Defect energetics for diffusion in CrMnFeCoNi high-entropy alloy from first-principles calculations," *Computational Materials Science,* vol. 170, 2019, doi: 10.1016/j.commatsci.2019.109163.

[13] S. Zhao, G. M. Stocks, and Y. Zhang, "Defect energetics of concentrated solid-solution alloys from ab initio calculations: Ni0.5Co0.5, Ni0.5Fe0.5, Ni0.8Fe0.2 and Ni0.8Cr0.2," *Phys Chem Chem Phys,* vol. 18, no. 34, pp. 24043-56, Sep 14 2016, doi: 10.1039/c6cp05161h.

[14] S. Zhao, T. Egami, G. M. Stocks, and Y. Zhang, "Effect of d electrons on defect properties in equiatomic NiCoCr and NiCoFeCr concentrated solid solution alloys," *Physical Review Materials,* vol. 2, no. 1, 2018, doi: 10.1103/PhysRevMaterials.2.013602.

[15] Y. Lu *et al.*, "A promising new class of irradiation tolerant materials: Ti2ZrHfV0.5Mo0.2 high-

entropy alloy," *Journal of Materials Science & Technology,* vol. 35, no. 3, pp. 369-373, 2019, doi: 10.1016/j.jmst.2018.09.034.

[16] K. Jin *et al.*, "Effects of compositional complexity on the ion-irradiation induced swelling and hardening in Ni-containing equiatomic alloys," *Scripta Materialia,* vol. 119, pp. 65-70, 2016, doi: 10.1016/j.scriptamat.2016.03.030.

[17] S. Zhao, "Defect properties in a VTaCrW equiatomic high entropy alloy (HEA) with the body centered cubic (bcc) structure," *Journal of Materials Science & Technology,* vol. 44, pp. 133-139, 2020, doi: 10.1016/j.jmst.2019.10.025.

[18] A. W. Carruthers *et al.*, "Novel reduced-activation TiVCrFe based high entropy alloys," *Journal of Alloys and Compounds,* vol. 856, 2021, doi: 10.1016/j.jallcom.2020.157399.

[19] M. R. Gilbert *et al.*, "Waste implications from minor impurities in European DEMO materials," *Nuclear Fusion,* vol. 59, no. 7, pp. 076015.1-076015.15, 2019.

[20] L. Tan *et al.*, "Design principles of low-activation high entropy alloys," *Journal of Alloys and Compounds,* vol. 907, 2022, doi: 10.1016/j.jallcom.2022.164526.

[21] H. Oh *et al.*, "Lattice Distortions in the FeCoNiCrMn High Entropy Alloy Studied by Theory and Experiment," *Entropy,* vol. 18, no. 9, 2016, doi: 10.3390/e18090321.

[22] A. Zunger, S. Wei, L. G. Ferreira, and J. E. Bernard, "Special quasirandom structures," *Phys Rev Lett,* vol. 65, no. 3, pp. 353-356, Jul 16 1990, doi: 10.1103/PhysRevLett.65.353.

[23] A. van de Walle *et al.*, "Efficient stochastic generation of special quasirandom structures," *Calphad,* vol. 42, pp. 13-18, 2013, doi: 10.1016/j.calphad.2013.06.006.

[24] C. Li *et al.*, "First principle study of magnetism and vacancy energetics in a near equimolar NiFeMnCr high entropy alloy," *Journal of Applied Physics,* vol. 125, no. 15, 2019, doi: 10.1063/1.5086172.

[25] G. Kresse and J. Hafner, "Ab initio molecular dynamics for liquid metals," *Physical review B,* vol. 47, no. 1, p. 558, 1993.

[26] G. Kresse and J. Furthmüller, "Efficient iterative schemes for ab initio total-energy calculations using a plane-wave basis set," *Physical review B,* vol. 54, no. 16, p. 11169, 1996.

[27] P. E. Blöchl, "Projector augmented-wave method," *Physical review B,* vol. 50, no. 24, p. 17953, 1994.

[28] G. Kresse and D. Joubert, "From ultrasoft pseudopotentials to the projector augmented-wave method," *Physical review b,* vol. 59, no. 3, p. 1758, 1999.

[29] J. P. Perdew, K. Burke, and M. Ernzerhof, "Generalized gradient approximation made simple," *Physical review letters,* vol. 77, no. 18, p. 3865, 1996.

[30] A. De Vita and M. Gillan, "The ab initio calculation of defect energetics in aluminium," *Journal of Physics: Condensed Matter,* vol. 3, no. 33, p. 6225, 1991.

[31] W. Chen *et al.*, "Vacancy formation enthalpies of high-entropy FeCoCrNi alloy via first-

principles calculations and possible implications to its superior radiation tolerance," *Journal of Materials Science & Technology,* vol. 34, no. 2, pp. 355-364, 2018, doi: 10.1016/j.jmst.2017.11.005.

[32] T. Shi *et al.*, "Distinct point defect behaviours in body-centered cubic medium-entropy alloy NbZrTi induced by severe lattice distortion," *Acta Materialia,* vol. 229, 2022, doi: 10.1016/j.actamat.2022.117806.

[33] G. Henkelman, B. P. Uberuaga, and H. Jónsson, "A climbing image nudged elastic band method for finding saddle points and minimum energy paths," *The Journal of chemical physics,* vol. 113, no. 22, pp. 9901-9904, 2000.

[34] P. Olsson, C. Domain, and J. Wallenius, "Ab initio study of Cr interactions with point defects in bcc Fe," *Physical Review B,* vol. 75, no. 1, 2007, doi: 10.1103/PhysRevB.75.014110.

[35] G. S. Was, *Fundamentals of radiation materials science: metals and alloys*. springer, 2016.

[36] Y. Zhang, A. Manzoor, C. Jiang, D. Aidhy, and D. Schwen, "A statistical approach for atomistic calculations of vacancy formation energy and chemical potentials in concentrated solid-solution alloys," *Computational Materials Science,* vol. 190, p. 110308, 2021.

[37] P. M. Derlet, D. Nguyen-Manh, and S. L. Dudarev, "Multiscale modeling of crowdion and vacancy defects in body-centered-cubic transition metals," *Physical Review B,* vol. 76, no. 5, 2007, doi: 10.1103/PhysRevB.76.054107.

[38] D. Nguyen-Manh, A. P. Horsfield, and S. L. Dudarev, "Self-interstitial atom defects in bcc transition metals: Group-specific trends," *Physical Review B,* vol. 73, no. 2, 2006, doi: 10.1103/PhysRevB.73.020101.

[39] W. Schilling, "Self-interstitial atoms in metals," *Journal of Nuclear Materials,* vol. 69, pp. 465-489, 1978.

[40] A. Schneider, C.-C. Fu, and C. Barreteau, "Local environment dependence of Mn magnetism in bcc iron-manganese alloys: A first-principles study," *Physical Review B,* vol. 98, no. 9, 2018, doi: 10.1103/PhysRevB.98.094426.